Published in final edited form as:
Magn Reson Med. 2008 February ; 59(2): 268–277. doi:10.1002/mrm.21487.

Quantitative Magnetic Resonance of *Post Mortem* Multiple Sclerosis Brain before and after Fixation

Klaus Schmierer, PhD[1], **Claudia AM Wheeler-Kingshott, PhD**[1], **Daniel J Tozer, PhD**[1], **Phil A Boulby, PhD**[1], **Harold G Parkes, PhD**[1], **Tarek A Yousry, Dr med habil, FRCR**[1], **Francesco Scaravilli, PhD, FRCPath**[2], **Gareth J Barker, PhD**[3], **Paul S Tofts, DPhil**[1,4], and **David H Miller, MD, FRCP**[1]

[1]NMR Research Unit, Institute of Neurology, University College London, London, United Kingdom

[2]Division of Neuropathology, Institute of Neurology, University College London, London, United Kingdom

[3]King's College London, Institute of Psychiatry, Department of Clinical Neurosciences, London, United Kingdom

Abstract

Unfixed and fixed *post mortem* multiple sclerosis (MS) brain is being used to probe pathology underlying quantitative MR (qMR) changes. Effects of fixation on qMR indices in MS brain are unknown. In 15 *post mortem* MS brain slices T_1, T_2, MT ratio (MTR), macromolecular proton fraction (f_B), mean, axial and radial diffusivity (MD, D_{ax} and D_{rad}), and fractional anisotropy (FA) were assessed in white matter (WM) lesions (WML) and normal appearing WM (NAWM) before and after fixation in formalin. Myelin content, axonal count and gliosis were quantified histologically. Student's t-test and regression were used for analysis. T_1, T_2, MTR, and f_B obtained in unfixed MS brain were similar to published values obtained in patients with MS *in vivo*. Following fixation T_1, T_2 (NAWM, WML) and MTR (NAWM) dropped, whereas f_B (NAWM, WML) increased. Compared to published *in vivo* data all diffusivity measures were lower in unfixed MS brain, and dropped further following fixation (except for FA). MTR was the best predictor of myelin in unfixed MS brain (r=−0.83; p<0.01) whereas post-fixation T_2 (r=0.92; p<0.01), T_1 (r=−0.89; p<0.01) and f_B (r=−0.86; p<0.01) were superior. All diffusivity measures (except for D_{ax} in unfixed tissue) were predictors of myelin content.

Introduction

Multiple Sclerosis (MS) is characterized by chronic inflammation and demyelination of the central nervous system. MR techniques are widely used to monitor the course of patients with MS. T_2-weighted and gadolinium (Gd) enhanced T_1-weighted MR images display MS white matter lesions (WML) with high sensitivity and are useful in diagnosis (1, 2). However, these MR measures correlate only modestly with disability (3, 4), in part because – aside from a relationship between Gd-enhancement and inflammation (5, 6) – they do not distinguish the other cardinal pathological substrates of MS: demyelination, remyelination, axonal loss and gliosis (7). Additional MR measures have been developed that are quantitative and potentially more pathologically specific. These include volumetric

Correspondence should be addressed to: Klaus Schmierer Box 117, NMR Research Unit, Institute of Neurology, University College London, Queen Square, London. WC1N 3BG. UK. Phone: +44 845 155 5000, ext 724470 Fax: +44 20 7278 5616 E-mail: k.schmierer@ion.ucl.ac.uk.
[4]Current address: Brighton and Sussex Medical School, Brighton, UK

measurements, magnetisation transfer (MT) imaging, quantitative measurement of T_1 and T_2, diffusion, and MR spectroscopic metabolite concentration measurement (8).

Investigation of *post mortem* tissue provides an opportunity to directly investigate the relationship between quantitative MR (qMR) measures and underlying pathology. With the intention to simulate as closely as possible the *in vivo* situation, some MR studies have been performed on unfixed brain tissue shortly following death. This type of study has been shown to be a useful approach to investigate the pathological correlates of four MR indices: T_1-hypointensity, quantitative T_1, MTR, and transverse magnetisation decay or short T_2 (9-13). So far only preliminary data have been produced about the pathological correlates of diffusion weighted MR imaging (DWI) in *post mortem* MS brain (14, 15).

In order to avoid structural damage due to autolysis short *post mortem* delays are desirable in MR-pathology correlation studies. However, considerable logistical efforts (and funding) are required to minimise the *post mortem* delay for acquisition of MRI using unfixed MS brain (16). Moreover, unfixed *post mortem* brain is very soft; hence it may be difficult to achieve accurate matching between regions of interest detected on MRI and in the tissue (17, 18), and the specimen is prone to be damaged due to manual handling. Apart from avoiding these disadvantages of unfixed brain, the use of fixed tissue enables archive material to be investigated and allows extended scanning times resulting in improved spatial resolution and signal-to-noise as compared to *in vivo* studies (19).

Several groups have explored the correlations between qMR changes and pathological indices in fixed *post mortem* MS brain (11) and spinal cord (20, 21). The interpretation of results in such studies may benefit from the systematic assessment of qMR changes following fixation. In the current study, we acquired maps from *post mortem* MS brain slices of 15 patients prior to and after formalin fixation for the following qMR parameters: T_1, T_2, two indices of MT (the macromolecular proton fraction [f_B] and MTR), mean, axial and radial diffusivity (MD, D_{ax} and D_{rad}, respectively) and fractional anisotropy (FA). The key aims of this study were to explore (i) the quantitative changes of these qMR measures following formalin fixation compared to data obtained prior to fixation, and (ii) whether the correlations between the qMR indices and quantitative histology measures are affected by these two conditions of the tissue (unfixed/fixed). Although qMR and histopathology data on unfixed tissue of some of the cases has been reported previously (13), it is necessary to present these findings again in order to allow the comparison between pre- and post-fixation qMR findings, which is the primary focus of the study.

Material and Methods

Patients

This study was approved by the Joint Ethics Committees of The National Hospital for Neurology and Neurosurgery and the Institute of Neurology, University College London. *Post mortem* brain slices of 15 patients with MS (14 women and one man) were provided by the UK Multiple Sclerosis Tissue Bank (MSTB) based at Charing Cross Hospital, Imperial College School of Medicine, London, UK. The mean age of the patients was 58 years (SD: 14 years; range: 34-82); their mean disease duration was 26 years (SD: 11; range: 6-49). Brains were retrieved by the MSTB a mean of 17 h (SD: 6 h; range: 7–28 h) after death.

The course of MS (22) and the disability of the patients were assessed retrospectively from the case records collected at the MSTB. Disability was estimated using the expanded disability status score (EDSS) scale (23). The patients' brain weight was provided by the MSTB.

Samples

Unfixed coronal *post mortem* brain slices (thickness: 1cm) of one cerebral hemisphere were obtained for this study. All brain slices were scanned twice, (i) under unfixed conditions 51 hours (SD: 28; range: 10-107) after death and (ii) after fixation in 10% formalin for 64 days (SD: 42; range: 8-133). The unfixed brain slices were sealed in plastic bags and stored in a refrigerator at 2-8°C until 3 hours before scanning when they were taken out of the fridge, wrapped in polyethylene film (to retain moisture) and left to warm up to scanner room temperature. Following MRI in unfixed condition, the specimens were immersed in 10% buffered formalin and kept at room temperature. For re-scanning they were taken out of the formalin bath and wrapped in polyethylene film again. The temperature of the specimens was monitored immediately after the last dataset (diffusion tensor imaging, DTI) had been acquired at each time point using a thermocouple thermometer (HI 93551) connected to a penetration probe (HPT1) from Hanna Instruments, Leighton Buzzard, Bedfordshire, UK.

MRI

The brain slices were scanned using the standard birdcage head coil of a GE Signa Horizon Echospeed 1.5 T system (General Electric, Milwaukee, WI, USA). The maximum gradient strength of this system was 22 mTm^{-1}. All MR sequences were acquired at a single slice location (thickness: 5 mm), centred in the middle, and parallel to the coronal surface of the specimen. Unless otherwise specified the following datasets were acquired using a matrix size of 256×256 and a field of view (FOV) of 24cm^2 (resulting in a pixel size of 0.94 mm^2):

- **i.** 2D dual spin echo proton density (PD)- and T_2-weighted (T_2w) images with parameters TR=2000 ms and TE = 30 or 120 ms, respectively. T_2 maps were calculated from the images using a two point fit of the data to the model $S = S_0\exp(-TE/T_2)$ (24). These data sets were acquired in all 15 cases before and after fixation.
- **ii.** 2D PD and T_1-weighted (T_1w) gradient echo images (TR/TE/flip angle: 1500ms/11ms/45° and 36ms/11ms/45°, respectively), from which T_1 maps were generated as previously described (13, 25). These datasets were acquired in unfixed condition in 15 cases, 14 of which were re-scanned after fixation.
- **iii.** 2D dual spin echo images (TR/TE1/TE2: 1720ms/30ms/80ms) obtained with (M_{sat}) and without (M_0) a saturation prepulse (16 ms, 23.2μT Hamming apodized 3 lobe sinc pulse, applied 1kHz from water resonance) from which MTR maps were calculated as $MTR = 100 \times (M_0 - M_{sat})/M_0$ (26). These datasets were acquired in all 15 cases before and after fixation.
- **iv.** 2D spoiled gradient echo images (TR/TE/flip angle: 1180ms/12ms/25°; FOV 240×180 with a partial *k* space coverage, reconstructed as 256×256 over a 24cm FOV). A Gaussian MT pulse of 14.6ms duration was applied at ten different combinations of MT pulse offsets and powers (three powers were used) as previously described (27). A model based on that of Henkelmann et al. (28), with modifications by Ramani et al. (29) to allow for pulsed rather than continuous MT saturation, was fitted to the data. The model allows calculation of six parameters (R_{1B}, RM_{0A}, gM_{0A}, $f_b/R_{1A}(1 - f_b)$, $1/R_{1A}T_{2A}$, and T_{2B}) which are combinations of the fundamental parameter f_B, R_{1A} and R_{1B} (the inverse of the T_1 of the A and B pools, respectively), R (the time constant for the interaction for the two pools), T_{2A} and T_{2B} (their transverse relaxation times), M_{0A} (the initial magnetisation of the A pool), and g (the scanner gain). With a separate measurement of R_{1A} (see below), f_B can be separately determined, although independent determination of the other interlinked parameters is not possible. These datasets were acquired prior to fixation in 10 samples, of which eight were re-scanned after fixation. A further four

samples were scanned only after fixation. Hence, altogether 12 samples were scanned in fixed condition. As MTR and f_B are percentages, and we also wish to calculate standard deviations as percentages of them, there is the potential ambiguity in using '%' or the phrase 'percent'. We therefore report MTR and f_B as 'percent units [pu]'. This measure (pu) is directly comparable to the 'percentage' (%) units reported by other groups, but does not suffer from this ambiguity (26).

v. multi-shot diffusion-weighted spin-echo EPI (DTI; TR/TE: 3000 / TE86ms). The gradient *b* factor was 1940smm^{-2}, number of shots= 8, NEX (i.e. signal averages)= 4 (acquired separately, and averaged after reconstruction), FOV= 12×12cm, matrix 48×48 (reconstructed as 64×64) resulting in a pixel size of 2.5×2.5mm^2 (reconstructed 1.9×1.9 mm^2). For each shot and average, six diffusion-weighted images along six non-co-linear directions, and one image with zero applied diffusion-sensitizing gradients (i.e. a T_2w (TE= 86ms) EPI scan with b~0) were acquired. The directions of the diffusion weighting were selected to apply maximum gradient strength along two axes at a time and to obtain a high *b* factor without increasing TE or losing signal-to-noise. The scheme used was (0 0 0, 1 1 0, 1 0 1, 0 1 1, −1 1 0, −1 0 1, 0 −1 1). Magnitude images of each slice were reconstructed and averaged off-line, prior to being processed to determine the diffusion tensor on a pixel-by-pixel basis. Mean, axial and radial diffusivity (MD, D_{ax} and D_{rad}, respectively) and FA were calculated from the principal eigenvalues of the diffusion tensor (30, 31). The largest eigenvalue obtained in each region of interest (ROI, see below) was considered to reflect D_{ax} whereas the remaining two eigenvalues were averaged and referred to as D_{rad} (32-35). This sequence was acquired in 13 cases before and after fixation, and in a further two cases only after fixation.

Total scanning time was 1 hour 45min for each scanning session.

Definition of ROI

All scans and maps were displayed on a Sun workstation (Sun Microsystems, Mountain View, CA, USA) using DispImage (36, 37). ROI in each case were identified in a stepwise process, starting from the T_2w SE images of the sample in unfixed condition. Here, ROI were defined as either (i) areas of hyper-intense signal suspected to be MS WML or (ii) regions of normal-appearing white matter (NAWM). Once ROI were marked on T_2w SE images they were transferred onto (inherently registered) T_1-, T_2- MTR-, and f_B-maps of the same case in unfixed condition, and values obtained. In the next step ROI on b~0 images (i.e. the T_2w EPI scans with zero applied diffusion-sensitizing gradients) in unfixed condition were identified by visually matching ROI observed on T_2w SE scans in unfixed condition with respective ROI on b~0 images. The latter ROI were then transferred onto (inherently registered) diffusivity- and FA-maps. Finally, ROI on SE T_2w scans and b~0 images following fixation were identified by visually matching them with the corresponding ROI on the respective SE T_2w scans and b~0 images of the specimen prior to fixation. qMR values were then obtained the same way as described in unfixed condition.

Correspondence between ROI detected on MRI and their histological substrates in brain slices was achieved using a previously described stereotactic procedure (18).

Pathological procedures

Tissue blocks sized approximately 1.5×1.5×1cm and containing the ROI detected on MRI were dissected. The blocks were cut in half using a 5mm deep iron angle resulting in two blocks of approximately 5mm thickness each with the cutting plane corresponding to the centre of the MRI plane. All dissected blocks were marked with notches at known positions,

usually on the ventral and lateral cut surfaces, in order to assure orientation in space after further processing. The blocks were processed for embedding in paraffin and sections stained with Haematoxylin & Eosin (H&E), Luxol-Fast blue (LFB) and Bielschowsky's silver impregnation (BIEL). Immunocytochemistry included antibodies to glial fibrillary acidic protein (GFAP, 1/1500), Myelin basic protein (MBP, 1/400), and CD68 (1/100; all from Dako, Glostrup, Denmark).

MS WML were defined in comparison to surrounding NAWM as clearly distinct, sharply demarcated areas of either myelin loss (demyelinated plaques) or of reduced myelin content with thinly myelinated axons throughout the WML (remyelinated plaques) (13, 38, 39). The lesion stage was categorized as either active (inflammation throughout the lesion), chronic active (hypocellular center, inflammation only at the rim of the WML), or chronic inactive (no inflammation) (13, 40, 41).

Quantitative histology was performed as previously described (13). In short, axon counts were estimated in WML and NAWM using a 21 bar quadrate grid graticule at a final magnification of ×1250. Myelin content and gliosis were quantified in WML and NAWM by assessing transmittance (T, defined as the transmitted light divided by the incident light) on sections stained for LFB (T_{myelin}) and GFAP ($T_{gliosis}$). A high value of T_{myelin} reflects low myelin content; a low value of $T_{gliosis}$ reflects more severe gliosis than high $T_{gliosis}$ (13).

The thickness of LFB- and GFAP-stained sections was assessed using a stereological microscope and a final magnification of ×787.5 in order to control for possible systematic errors in the measurements of T (13).

Statistical Methods

To compare variables in WML versus NAWM, the Student's paired t-test was used on patient means averaged over respective tissue compartments (WML, NAWM). Associations between MR indices before and after fixation were performed using linear regression, applied to patient means over respective tissue compartments resulting in two data points (WML, NAWM) per patient. Linear regression was also used to test for correlations between MR indices and axonal count, myelin content and gliosis. To investigate confounding of the pair-wise associations by other variables, these were entered as covariates into the regression. Statistical significance was assumed when $p<0.05$. The analysis was carried out using SPSS version 11.5 (SPSS, Chicago, IL, USA).

Results

The clinical course had been secondary progressive in eight subjects and primary progressive in two. In five subjects, the clinical course could not be determined. The estimated mean EDSS before death was 8 (SD: 1.1; median: 8.5; range: 6.5 – 9) and mean brain weight 1126g (SD: 100g, range: 1000 – 1300g).

Lesion findings

Between one and seven WML in each brain slice (mean 3.4 WML; SD: 1.8 WML; median: 3 WML) could be used for analysis. In total, 51 histologically confirmed MS WML were identified on T_2w MRI of 15 cases under unfixed conditions. Fourty-four/51 WML (86.3 %) were visible using the same T_2w sequence after formalin fixation. MR data were also obtained from one to three NAWM ROI in each slice, and averaged to produce a single NAWM value, before and after fixation.

Of 13/15 brain slices DTI data were acquired under unfixed conditions. In these 13 unfixed brain slices 44 histologically confirmed WML were detected on T_2w MRI. Thirty-three/44

WML (75%) were visible on b_0 images (unfixed). Of the 33 WML detected on b~0 images of unfixed brain slices, 27 (81.8%) were visible using the same sequence after fixation.

DTI data after fixation were obtained of all 15 cases included in this study. In total 33 histologically confirmed WML were detected on the b~0 images. These 33 WML account for 75% of the 44 WML detected on T_2w MRI after fixation and for 64.7% of the 51 WML detected on T_2w MRI in unfixed condition.

Forty-eight/51 WML (94.1%) were demyelinated and three remyelinated (5.9%). In three/48 demyelinated WML small areas of remyelination at the lesion edges were seen; because these areas covered less than 10% of the whole WML, the lesions were classified as demyelinated (13).

Comparison of MS WML and NAWM (table 1)

All quantitative MR indices differed significantly between WML and NAWM before as well as after fixation. Histologically, T_{myelin} in WML was higher (indicating lower myelin content) than in NAWM. Compared to NAWM there was significantly more axonal loss and lower $T_{gliosis}$ (indicating more severe gliosis) in WML.

MR indices before and after fixation (table 2, figure 1)

Fixation of the brain tissue led to significant reductions in T_1 and T_2 (WML, NAWM), MTR (NAWM), MD (NAWM), D_{ax} and D_{rad} (WML, NAWM) whereas f_B increased in NAWM and WML. Marginally significant reductions were detected for MD and FA in WML. No significant changes were detected for MTR in WML and for FA in NAWM.

Correlation of MR indices and pathology

Unfixed tissue (table 3)—T_{myelin} (inversely related to myelin content) correlated strongly with MTR (r= −0.83, p<0.01), slightly less so with T_1, T_2, f_B, MD, FA, and D_{rad}. T_2 and MTR were also strongly associated with axonal count. Moderate correlations were detected between axonal count and both T_1 and f_B.

Fixed tissue (table 4)—T_{myelin} (inversely related to myelin content) correlated strongly with T_1, T_2, f_B, FA, D_{ax} and D_{rad} as did T_1 with axonal count. MD and MTR correlated moderately with myelin content, as did f_B and FA with axonal count and MTR with gliosis.

Correlation between neuropathological features (table 4)

T_{myelin} (inversely related to myelin content) was strongly associated with axonal count (r= −0.8, p<0.01) and weakly with gliosis.

Analysis of confounding correlations

MR acquired in unfixed condition—Multivariate regression revealed the following primary and secondary associations: When T_{myelin} was regressed on MTR and f_B simultaneously, the association between MTR and T_{myelin} remained significant (partial r= −0.64; p=0.02) whereas the correlation between f_B and T_{myelin} disappeared (partial r= −0.19; p=0.47). When T_{myelin} was regressed on MTR and T_1 simultaneously the association between MTR and T_{myelin} remained robust (partial r= −0.6; p<0.01) whereas the correlation between T_1 and T_{myelin} lost significance (partial r= 0.30; p=0.08). When T_{myelin} was regressed on MTR and T_2 simultaneously the association between MTR and T_{myelin} remained significant (partial r= −0.48; p=0.03) whereas the correlation between T_2 and T_{myelin} did not. These data suggest that in unfixed MS brain the association between (i)

T_{myelin} and T_1, (ii) T_{myelin} and T_2, and (iii) T_{myelin} and f_B is secondary to the correlation between T_{myelin} and MTR.

When MTR was regressed on axonal count and T_{myelin} simultaneously, only a weak association between MTR and axonal count was detected, while MTR remained significantly correlated with T_{myelin} (partial r=−0.54, p<0.01; partial r for MTR versus axonal count: 0.37, P=0.04). This suggests that the association between MTR and axonal count results from the strong correlation of myelin content with (i) axonal count and (ii) MTR.

FA, MD and D_{rad} were all primarily predictors of myelin content (partial r for FA versus T_{myelin}:−0.8, p<0.01; partial r for FA versus axonal count: −0.04, p=0.85; partial r for MD versus T_{myelin}=0.82, p<0.01; partial r for MD versus axonal count: 0.12, p=0.6; partial r for D_{rad} versus T_{myelin}: 0.8, p<0.01; partial r for D_{rad} versus axonal count: 0.07, p=0.74). Regression of D_{ax} on both T_{myelin} and axonal count resulted in a loss of the relationship between D_{ax} and either of the two histological indices.

When T_{myelin} was regressed on MD and FA simultaneously, the correlation between both MR indices and T_{myelin} remained significant, suggesting that neither of these measures emerges as the single predictor, which was also true for simultaneous regression of T_{myelin} on FA and D_{rad}. Multivariate regression did not reveal any further meaningful correlations.

MR acquired in fixed condition—T_2, T_1 and f_B were all strong predictors of myelin content. When T_{myelin} was regressed on these three qMR indices simultaneously, the association between T_2 and T_{myelin} remained strong (partial r= 0.65; p=0.01), whereas the correlation between the remaining two indices and T_{myelin} lost significance. These data suggests that in fixed *post mortem* tissue T_2 is the strongest predictor of myelin content.

When T_2 was regressed on axonal count and T_{myelin} simultaneously, the association between T_2 and axonal count disappeared, while T_2 remained strongly correlated with T_{myelin} (partial r= 0.85, p<0.01). This suggests that the association between T_2 and axons results from the strong correlation between axonal count and myelin content and between T_2 and T_{myelin}.

All DTI indices were primarily predictors of myelin content. Whilst there was overall strong correlation among these indices with each other (table 4), there was statistical evidence for FA to be the single best predictor (data not shown).

No confounding effects were detected between any of the detected correlations and estimated EDSS, age, disease duration, temperature of the specimen during the scanning experiments, or time between (i) death and tissue retrieval and (ii) death and MRI (unfixed and fixed). To further test for possible confounding of qMR data after fixation (42) through short fixation times we excluded four cases in our sample with a fixation time less than 45 days (mean fixation time 14 days, SD: 6 days). No significant difference was detected in the remaining 11 cases when compared with the entire sample for any of the qMR data obtained before and after fixation or for the regression analysis of associations between indices.

Discussion

The key findings of this study are:

1. Formalin fixation of *post mortem* MS brain led to significant changes of all qMR indices investigated in this study with some variation in the magnitude of change between (i) MR modalities and (ii) WML and NAWM.

2. All indices were primarily dependent on myelin content. None of the MR indices was a primary predictor of axonal count or gliosis.
3. MTR was the best predictor of myelin content in unfixed MS brain whereas following fixation T_2 appeared to be superior to T_1, f_B and MTR.
4. Despite an overall significantly reduced diffusivity (compared to *in vivo* measurements) all DTI indices (except for D_{ax}) were robust predictors of myelin in *post mortem* brain, prior to and after fixation.

The molecular mechanism of tissue fixation is not well understood. It is thought that formaldehyde solutions react with various functional groups of macromolecules in a cross-linking fashion. Among the most reactive sites are primary amines (e.g. lysine) and thiols (e.g. cystein). Subsequently, these functional groups may bind to less reactive groups including primary amides (e.g. glutamine), guanidine groups (arginine) and thyrosine ring carbons. This intra- and intermolecular cross-linking of macromolecules alters the physical characteristics of tissues (43). The result is a gel that largely retains the cellular constituents in their *in vivo* relationships to each other (44). Distortion of brain tissue following fixation may, however, occur and shrinkage by up to ~19% following fixation using 10% formalin solution has been observed (45).

Standard MR acquisition and processing protocols were employed in this study to obtain T_2w images as well as T_1, T_2 and MT datasets. More than 85% of WML detected on T_2w scans of unfixed tissue were also detected using the same sequence after fixation. The decreased sensitivity of T_2w MRI sequences optimized for *in vivo* detection of WML in MS brain following fixation has been observed before (18), and may be due to a reduction of T_2 following formalin fixation (46-48), the fixative itself (49), distortion of the tissue (45), and a slight difference of the imaging plane between the scans under fresh and fixed conditions (18).

Though MR acquisition in this study was performed on specimens at room temperature (~22.5°C), the values of T_1, T_2, MTR and f_B in unfixed *post mortem* NAWM were similar to those detected *in vivo* (24, 27, 50). However, significant changes occurred following fixation (table 2). The pattern of these changes is in line with the concepts of (i) a reduction in T_1 and T_2 due to formalin in aqueous solution (49) and (ii) the action formalin exerts on tissue (cross-linking of macromolecules) leading to a shift of protons from the free to the macromolecular pool which may result in a shortening of T_1 (46-47). The latter effect would also impact on MT: As MTR can be described – in a simplistic model – as $MTR = f_B * T_1 * k$ (where k is a constant) (51), it is not unexpected that MTR is reduced, too. f_B, on the other hand, is thought to reflect protons in the macromolecular proton pool only (51-52), and this pool may be increased in the process of fixation due to protons in soluble macromolecules becoming protons in insoluble macromolecules. These changes may also explain why the correlation of MTR and T_{myelin} is reduced in fixed tissue. As the f_B and T_1 changes following fixation are in opposite directions it does not seem surprising that the composite measure's correlation with T_{myelin} is reduced. The investigation of fixation-effects on brain tissue could further be improved by washing the tissue in buffered saline following fixation and prior to scanning, thereby reducing the effect of the fixative itself on MR indices (49). Moreover, it has been reported that following immersion of brain tissue in fixative T_1, T_2 and spin density may require over five weeks to stabilize (42). Although in our sample time of fixation did not seem to affect the qMR data obtained, a standardized interval between immersion in fixative and MR acquisition of at least five weeks would be advisable (42, 48).

DTI of *post mortem* MS brain revealed significantly reduced diffusivity indices even in unfixed conditions. Compared to values obtained *in vivo*, MD was reduced in NAWM *post mortem* by well over two third (from 0.84 to 0.22×10^{-3} mm^2/s) and FA by about one third

(from 0.62 to 0.40) (53). Following fixation the diffusivity indices – except for FA – were reduced even further (table 2). Factors which affect molecular/cellular structure and that may have contributed to these reductions include dehydration of the tissue, the lower than *in vivo* temperature during MRI, the failure of energy dependent ion transport mechanisms in *post mortem* samples (19, 54, 55) and – following fixation – the formation of cross links between amino acid residues as well as some degree of shrinkage (45).

The reduced diffusivity in the *post mortem* brain required a different sequence optimisation compared to an *in vivo* protocol. Multi-shot (instead of single-shot) EPI was used to reduce image distortions, and a *b* factor almost twice the value used *in vivo* was chosen to accommodate for the reduced diffusion coefficient in the *post mortem* brain (56). An even greater *b* factor of ~4000smm^{-2} would likely result in an even better sensitivity to white matter changes at low FA values (57).

This study confirms that in unfixed *post mortem* brain of MS patients, MTR is a robust index of myelin content (10, 12, 13). The correlation of T_{myelin} with f_B, T_1, T_2 and DTI indices (with the exception of D_{ax}) was also strong (table 3). However, multivariate regression revealed that, when MR data were acquired in unfixed brain, the primary correlation emerged between myelin content and MTR, whereas the other qMR indices were only secondarily associated with myelin content.

All qMR indices investigated were clearly different between WML and NAWM, regardless of whether they were acquired in unfixed brain or after fixation (table 1). However, formalin fixation altered some of the relationships between qMR and histology indices, with changes in the two MT indices being most apparent: Firstly, the correlation of MTR with myelin content dropped substantially (unfixed r=−0.831, p<0.001; fixed r=−0.681, p<0.001). Secondly, after fixation f_B was (i) significantly higher in WML as well as in NAWM, suggesting a net shift of protons from the mobile to the macromolecular pool following fixation and (ii) more strongly associated with myelin content than when assessed in unfixed tissue (tables 3 and 4).

After fixation T_2 emerged as the strongest predictor of myelin content. This finding is in agreement with a *post mortem* study of MS spinal cord, where out of three indices (MTR, T_1, T_2) T_2 showed the strongest association with myelination status (21). It should be noted, however, that the assessment of T_2 and its correlation with histological features in the current study was a ‘by-product’ of the dual echo sequence employed to collect T_2w images. Neither precise measurements of T_2 employing a multi-echo sequence (58) nor multi-exponential T_2 decay curve analysis (50, 59) were performed in this study. Nevertheless, our results as well as reports by others (12, 60) should encourage further studies to clarify the potential of quantitative measures of T_2 relaxation as a predictor of myelin in MS brain.

None of the investigated MR indices was primarily associated with axonal count, either before or after fixation. These results confirm and extend earlier findings that suggested the association between axonal count and MTR (and T_1) as being secondary to the correlation of these qMR measures with myelin content (12, 13). Variations in myelin content appear to result in changes in the concentration and mobility of protons that have a stronger influence on MT- and DTI- derived measures than do changes in the number of axons.

According to the two pool model of MT, f_B is thought to reflect an absolute measure of the amount of macromolecular protons (i.e. the semisolid pool of protons) (51-52). The current study provides histo-pathological evidence that f_b indeed primarily reflects protons associated with myelin (27, 50). The strong association of f_B with myelin content in the *post mortem* MS brain in both unfixed and fixed conditions also suggests that useful conclusions about *in vivo* changes may be inferred from data acquired using fixed tissue. Whether it is

worthwhile to use tissue that has been fixed over longer term, will require further investigation. In the current study only tissue that was fixed for, on average, two months has been included.

As previously discussed (13), despite the strong association shown in *post mortem* MS brain between measures of MT and myelin content, abnormalities in the former may not solely be due to variations in the latter (61) as (i) MTR includes MT and direct saturation effects, both of which depend on sequence parameters (62-65), (ii) the degree of direct saturation caused by the MT prepulse (66) depends on intrinsic properties such as the T_1 of the free water and the width of the free water peak, which will vary between tissues and (iii) the MT effect itself depends not only on the presence of two (or more) proton pools, but also on the exchange rate between the pools, which may in turn vary with pH, temperature and pathology (67). Moreover, f_B may be affected by macromolecules other than myelin and by processes such as inflammation (which could lead to changes in the fraction of free water).

In our sample of chronic *post mortem* MS brain all investigated DTI indices (except for D_{ax}) were primarily affected by myelin content. This finding is broadly in agreement with an earlier *post mortem* study of the spinal cord using a 7T system, though multivariate analysis was not performed in that study (68).

In conclusion, all qMR measures investigated in this study appear to be useful tools to assess MS pathology in *post mortem* MS brain and – by inference – *in vivo*. In unfixed *post mortem* tissue, MTR appeared to be the most robust index of myelin content, followed by T_2, T_1, f_B, and FA. However, when scanned after fixation T_1 and f_B and particularly T_2 emerged as the strongest predictors of myelin content. All three indices also correlated strongly with myelin content in unfixed tissue suggesting that they may be advantageous when qMR assessment of fixed MS brain are used to infer likely *in vivo* changes. The loss after fixation of the strong association between MTR and myelin observed pre-fixation serves as a warning that MR-pathology correlation studies using post-fixation qMR measures may not be reliable when interpreting the pathological basis of *in vivo* qMR measures. On the other hand, the consistent correlation obtained between MTR and myelin content in unfixed tissue using both univariate and multivariate analyses suggests that MTR, measured using the sequence applied in the present study, is likely to be a reliable measure of myelination in MS white matter *in vivo*. DTI indices also provide a consistent assessment of myelin content before and after fixation. However, whereas the absolute values of T_1, T_2, and f_B appear to remain rather stable after death, DTI indices – with the relative exception of FA – drop substantially (19, 55), perhaps making it less straightforward to infer likely *in vivo* changes from *post mortem* observations.

None of the investigated qMR indices was a primary predictor of axonal count or gliosis, both important aspects of MS histology for which non-invasive tools are urgently needed in order to improve natural history studies and the assessment of treatments aimed at influencing these features.

Acknowledgments

We thank the UK Multiple Sclerosis Tissue Bank (MSTB) for providing tissue samples for this study, Ros Gordon, Christopher Benton, and David G MacManus for expert radiographic assistance, Gerard R Davies, Michael J Groves and Tamas Revesz for helpful discussions, and Stephen Dawodu, Derek Marsdon, Steve Duerr, and Waqar Rashid for technical support. Special thanks to Dr Daniel R Altmann for statistical support. KS is a Wellcome Trust Intermediate Clinical Fellow (grant #075941). HGP is also supported by the Wellcome Trust. The stereotactic system was funded by the Sir Jules Thorn Charitable Trust (grant #03SC/08A). PAB was funded by Action Research. The NMR Research Unit and the MSTB are supported by the Multiple Sclerosis Society of Great Britain & Northern Ireland, which also funded CAMWK, GJB and DJT.

References

1. Miller DH. Biomarkers and surrogate outcomes in neurodegenerative disease: lessons from multiple sclerosis. NeuroRx. 2004; 1:284–294. [PubMed: 15717029]
2. Polman CH, Reingold SC, Edan G, Filippi M, Hartung HP, Kappos L, Lublin FD, Metz LM, McFarland HF, O'Connor PW, Sandberg-Wollheim M, Thompson AJ, Weinshenker BG, Wolinsky JS. Diagnostic criteria for multiple sclerosis: 2005 revisions to the “McDonald Criteria”. Ann Neurol. 2005; 58:840–846. [PubMed: 16283615]
3. Kappos L, Moeri D, Radue EW, Schoetzau A, Schweikert K, Barkhof F, Miller D, Guttmann CR, Weiner HL, Gasperini C, Filippi M. Predictive value of gadolinium-enhanced magnetic resonance imaging for relapse rate and changes in disability or impairment in multiple sclerosis: a meta-analysis. Lancet. 1999; 353:964–969. [PubMed: 10459905]
4. Brex PA, Ciccarelli O, O'Riordan JI, Sailer M, Thompson AJ, Miller DH. A longitudinal study of abnormalities on MRI and disability from multiple sclerosis. N Engl J Med. 2002; 346:158–164. [PubMed: 11796849]
5. Hawkins CP, Munro PM, Mackenzie F, Kesselring J, Tofts PS, Du Boulay EP, Landon DN, McDonald WI. Duration and selectivity of blood-brain barrier breakdown in chronic relapsing experimental allergic encephalomyelitis studied by gadolinium-DTPA and protein markers. Brain. 1990; 113:365–378. [PubMed: 2328409]
6. Katz D, Taubenberger JK, Cannella B, McFarlin DE, Raine CS, McFarland HF. Correlation between magnetic resonance imaging findings and lesion development in chronic, active multiple sclerosis. Ann Neurol. 1993; 34:661–669. [PubMed: 8239560]
7. Moore GRW. MRI-clinical correlations: more than inflammation alone - what can MRI contribute to improve the understanding of pathological processes in MS? J Neurol Sci. 2003; 206:175–179. [PubMed: 12559507]
8. Tofts, PS., editor. Quantitative MRI of the brain: Measuring changes caused by disease. 1 ed.. Chichester: Wiley; 2003.
9. van Walderveen MAA, Kamphorst W, Scheltens P, van Waesberghe JH, Ravid R, Valk J, Polman CH, Barkhof F. Histopathologic correlate of hypointense lesions on T1-weighted spin-echo MRI in multiple sclerosis. Neurology. 1998; 50:1282–1288. [PubMed: 9595975]
10. van Waesberghe JH, Kamphorst W, de Groot CJ, van Walderveen MAA, Castelijns JA, Ravid R, Nijeholt GJ, van der Valk P, Polman CH, Thompson AJ, Barkhof F. Axonal loss in multiple sclerosis lesions: magnetic resonance imaging insights into substrates of disability. Ann Neurol. 1999; 46:747–754. [PubMed: 10553992]
11. Moore GRW, Leung E, MacKay AL, Vavasour IM, Whittall KP, Cover KS, Li DK, Hashimoto SA, Oger J, Sprinkle TJ, Paty DW. A pathology-MRI study of the short-T2 component in formalin-fixed multiple sclerosis brain. Neurology. 2000; 55:1506–1510. [PubMed: 11094105]
12. Barkhof F, Brück W, de Groot CJ, Bergers E, Hülshof S, Geurts J, Polman CH, van der Valk P. Remyelinated lesions in multiple sclerosis: magnetic resonance image appearance. Arch Neurol. 2003; 60:1073–1081. [PubMed: 12925362]
13. Schmierer K, Scaravilli F, Altmann DR, Barker GJ, Miller DH. Magnetization transfer ratio and myelin in postmortem multiple sclerosis brain. Ann Neurol. 2004; 56:407–415. [PubMed: 15349868]
14. Fox R, Holtman R, Lee JC, Tkach J, Phillips M, Fisher E. Diffusion tensor measurements in post-mortem brain [abstract]. Proc Int Soc Magn Reson Med. 2005; 13:139.
15. Schmierer K, Wheeler-Kingshott CAM, Scaravilli F, Boulby PA, Miller DH. Diffusion tensor indices and their histological correlates in *post mortem* multiple sclerosis brain [abstract]. Proc Int Soc Magn Reson Med. 2005; 13:70.
16. Bö L, Geurts JJ, Ravid R, Barkhof F. Magnetic resonance imaging as a tool to examine the neuropathology of multiple sclerosis. Neuropathol Appl Neurobiol. 2004; 30:106–117. [PubMed: 15043708]
17. Newcombe J, Hawkins CP, Henderson CL, Patel HA, Woodroofe MN, Hayes GM, Cuzner ML, MacManus D, Du Boulay EP, McDonald WI. Histopathology of multiple sclerosis lesions

detected by magnetic resonance imaging in unfixed postmortem central nervous system tissue. Brain. 1991; 114:1013–1023. [PubMed: 2043938]

18. Schmierer K, Scaravilli F, Barker GJ, MacManus DG, Miller DH. Stereotactic co-registration of magnetic resonance imaging and histopathology in post-mortem multiple sclerosis brain. Neuropath Appl Neurobiol. 2003; 29:596–601. [PubMed: 14636166]
19. Sun SW, Neil JJ, Song SK. Relative indices of water diffusion anisotropy are equivalent in live and formalin-fixed mouse brains. Magn Reson Med. 2003; 50:743–748. [PubMed: 14523960]
20. Nijeholt GJ, Bergers E, Kamphorst W, Bot J, Nicolay K, Castelijns JA, van Waesberghe JH, Ravid R, Polman CH, Barkhof F. Post-mortem high-resolution MRI of the spinal cord in multiple sclerosis: a correlative study with conventional MRI, histopathology and clinical phenotype. Brain. 2001; 124:154–166. [PubMed: 11133795]
21. Bot JC, Blezer EL, Kamphorst W, Lycklama ANG, Ader HJ, Castelijns JA, Ig KN, Bergers E, Ravid R, Polman C, Barkhof F. The spinal cord in multiple sclerosis: relationship of high-spatial-resolution quantitative MR imaging findings to histopathologic results. Radiology. 2004; 233:531–540. [PubMed: 15385682]
22. Lublin FD, Reingold SC. Defining the clinical course of multiple sclerosis: results of an international survey. Neurology. 1996; 46:907–911. [PubMed: 8780061]
23. Kurtzke JF. Rating neurologic impairment in multiple sclerosis: an expanded disability status scale (EDSS). Neurology. 1983; 33:1444–1452. [PubMed: 6685237]
24. Boulby, PA.; Rugg-Gunn, F. T2: the transverse relaxation time. In: Tofts, PS., editor. Quantitative MRI of the brain. Measuring changes caused by disease. Chichester: John Wiley & Sons Ltd; 2003. p. 143-201.
25. Parker GJM, Barker GJ, Tofts PS. Accurate multislice gradient echo T(1) measurement in the presence of non-ideal RF pulse shape and RF field nonuniformity. Magn Reson Med. 2001; 45:838–845. [PubMed: 11323810]
26. Barker GJ, Tofts PS, Gass A. An interleaved sequence for accurate and reproducible clinical measurement of magnetization transfer ratio. Magn Reson Imaging. 1996; 14:403–411. [PubMed: 8782178]
27. Davies GR, Tozer DJ, Cercignani M, Ramani A, Dalton CM, Thompson AJ, Barker GJ, Tofts PS, Miller DH. Estimation of the macromolecular proton fraction and bound pool T2 in multiple sclerosis. Mult Scler. 2004; 10:607–613. [PubMed: 15584482]
28. Henkelman RM, Huang X, Xiang QS, Stanisz GJ, Swanson SD, Bronskill MJ. Quantitative interpretation of magnetization transfer. Magn Reson Med. 1993; 29:759–766. [PubMed: 8350718]
29. Ramani A, Dalton C, Miller DH, Tofts PS, Barker GJ. Precise estimate of fundamental in-vivo MT parameters in human brain in clinically feasible times. Magn Reson Imaging. 2002; 20:721–731. [PubMed: 12591568]
30. Pierpaoli C, Basser PJ. Toward a quantitative assessment of diffusion anisotropy. Magn Reson Med. 1996; 36:893–906. [PubMed: 8946355]
31. Basser PJ, Pierpaoli C. A simplified method to measure the diffusion tensor from seven MR images. Magn Reson Med. 1998; 39:928–934. [PubMed: 9621916]
32. Basser PJ. Inferring microstructural features and the physiological state of tissues from diffusion-weighted images. NMR Biomed. 1995; 8:333–344. [PubMed: 8739270]
33. Basser PJ, Pajevic S, Pierpaoli C, Duda J, Aldroubi A. *In vivo* fiber tractography using DT-MRI data. Magn Reson Med. 2000; 44:625–632. [PubMed: 11025519]
34. Xue R, van Zijl PC, Crain BJ, Solaiyappan M, Mori S. *In vivo* three-dimensional reconstruction of rat brain axonal projections by diffusion tensor imaging. Magn Reson Med. 1999; 42:1123–1127. [PubMed: 10571934]
35. Song SK, Sun SW, Ramsbottom MJ, Chang C, Russell J, Cross AH. Dysmyelination revealed through MRI as increased radial (but unchanged axial) diffusion of water. NeuroImage. 2002; 17:1429–1436. [PubMed: 12414282]
36. Plummer DL. Dispimage: a display and analysis tool for medical images. Rev Neuroradiol. 1992; 5:489–495.

37. Grimaud J, Lai M, Thorpe J, Adeleine P, Wang L, Barker GJ, Plummer DL, Tofts PS, McDonald WI, Miller DH. Quantification of MRI lesion load in multiple sclerosis: a comparison of three computer-assisted techniques. Magn Reson Imaging. 1996; 14:495–505. [PubMed: 8843362]
38. Prineas, JW.; McDonald, WI.; Franklin, RJM. Demyelinating diseases. In: Graham, DI.; Lantos, PC., editors. Greenfield's neuropathology. 7 ed.. London: Arnold; 2002. p. 471-550.
39. Brück W, Kuhlmann T, Stadelmann C. Remyelination in multiple sclerosis. J Neurol Sci. 2003; 206:181–185. [PubMed: 12559508]
40. Trapp BD, Peterson J, Ransohoff RM, Rudick R, Mörk S, Bö L. Axonal transection in the lesions of multiple sclerosis. N Engl J Med. 1998; 338:278–285. [PubMed: 9445407]
41. van der Valk P, de Groot CJ. Staging of multiple sclerosis (MS) lesions: pathology of the time frame of MS. Neuropathol Appl Neurobiol. 2000; 26:2–10. [PubMed: 10736062]
42. Yong-Hing CJ, Obenaus A, Stryker R, Tong K, Sarty GE. Magnetic resonance imaging and mathematical modelling of progressive formalin fixation of the human brain. Magn Reson Med. 2005; 54:324–332. [PubMed: 16032673]
43. Fox CH, Johnson FB, Whiting J, Roller PP. Formaldehyde fixation. J Histochem Cytochem. 1985; 33:845–853. [PubMed: 3894502]
44. Hopwood, D. Fixation and fixatives. In: Bancroft, JD.; Stevens, A., editors. Theory and practice of histological techniques. 4 ed.. New York: Churchill Livingstone; 1996. p. 23-45.
45. Mouritzen Dam A. Shrinkage of the brain during histological procedures with fixation in formaldehyde solutions of different concentrations. J Hirnforsch. 1979; 20:115–119. [PubMed: 556570]
46. Nagara H, Inoue T, Koga T, Kitaguchi T, Tateishi J, Goto I. Formalin fixed brains are useful for magnetic resonance imaging (MRI) study. J Neurol Sci. 1987; 81:67–77. [PubMed: 3681342]
47. Macchi G, Cioffi RP. An in vivo and post mortem MRI study in multiple sclerosis with pathological correlation. Ital J Neurol Sci. 1992; 13(9 Suppl 14):97–103. [PubMed: 1345748]
48. Blamire AM, Rowe JG, Styles P, McDonald B. Optimising imaging parameters for post mortem MR imaging of the human brain. Acta Radiol. 1999; 40:593–597. [PubMed: 10598845]
49. Bossart EL, Inglis BA, Silver XS, Mareci TH. The effect of fixative solutions in magnetic resonance imaging [abstract]. Proc Int Soc Magn Reson Med. 1999; 7:1928.
50. Tozer DJ, Davies GR, Altmann DR, Miller DH, Tofts PS. Correlation of apparent myelin measures obtained in multiple sclerosis patients and controls from magnetization transfer and multicompartmental T2 analysis. Magn Reson Med. 2005; 53:1415–1422. [PubMed: 15906291]
51. Tofts, PS.; Steens, SCA.; van Buchem, MA. MT: Magnetization transfer. In: Tofts, PS., editor. Quantitative MRI of the brain. Measuring changes caused by disease. Chichester: John Wiley & Sons Ltd; 2003. p. 257-298.
52. Sled JG, Pike GB. Quantitative imaging of magnetization transfer exchange and relaxation properties *in vivo* using MRI. Magn Reson Med. 2001; 46:923–931. [PubMed: 11675644]
53. Ciccarelli O, Werring DJ, Wheeler-Kingshott CA, Barker GJ, Parker GJ, Thompson AJ, Miller DH. Investigation of MS normal-appearing brain using diffusion tensor MRI with clinical correlations. Neurology. 2001; 56:926–933. [PubMed: 11294931]
54. Le Bihan D, Turner R, Douek P, Patronas N. Diffusion MR imaging: clinical applications. Am J Roentgenol. 1992; 159:591–599. [PubMed: 1503032]
55. Lee VM, Burdett NG, Carpenter TA, Herrod NJ, James MF, Hall LD. Magnetic resonance imaging of the common marmoset head. ATLA. 1998; 26:343–356.
56. Wheeler-Kingshott CAM, Schmierer K, Ciccarelli O, Boulby PA, Parker GJM, Miller DH. Diffusion tensor imaging of *post-mortem* brain (fresh and fixed) on a clinical scanner [abstract]. Proc Int Soc Magn Reson Med. 2003; 11:422.
57. Jones DK, Horsfield MA, Simmons A. Optimal strategies for measuring diffusion in anisotropic systems by magnetic resonance imaging. Magn Reson Med. 1999; 42:515–525. [PubMed: 10467296]
58. Whittall KP, MacKay AL, Li DK. Are mono-exponential fits to a few echoes sufficient to determine T2 relaxation for in vivo human brain? Magn Reson Med. 1999; 41:1255–1257. [PubMed: 10371459]

59. MacKay A, Whittall K, Adler J, Li D, Paty D, Graeb D. In vivo visualization of myelin water in brain by magnetic resonance. Magn Reson Med. 1994; 31:673–677. [PubMed: 8057820]
60. Laule C, Leung E, Lis DK, Traboulsee AL, Paty DW, MacKay AL, Moore GRW. Myelin water imaging in multiple sclerosis: quantitative correlations with histopathology. Mult Scler. 2006; 12:747–753. [PubMed: 17263002]
61. Odrobina EE, Lam TY, Pun T, Midha R, Stanisz GJ. MR properties of excised neural tissue following experimentally induced demyelination. NMR Biomed. 2005; 18:277–284. [PubMed: 15948233]
62. Stanisz GJ, Kecojevic A, Bronskill MJ, Henkelman RM. Characterizing white matter with magnetization transfer and T(2). Magn Reson Med. 1999; 42:1128–1136. [PubMed: 10571935]
63. Henkelman RM, Stanisz GJ, Graham SJ. Magnetization transfer in MRI: a review. NMR Biomed. 2001; 14:57–64. [PubMed: 11320533]
64. Berry I, Barker GJ, Barkhof F, Campi A, Dousset V, Franconi JM, Gass A, Schreiber W, Miller DH, Tofts PS. A multicenter measurement of magnetization transfer ratio in normal white matter. J Magn Reson Imaging. 1999; 9:441–446. [PubMed: 10194715]
65. Tofts PS, Steens SC, Cercignani M, Admiraal-Behloul F, Hofman PA, van Osch MJ, Teeuwisse WM, Tozer DJ, Van Waesberghe JH, Yeung R, Barker GJ, van Buchem MA. Sources of variation in multi-centre brain MTR histogram studies: body-coil transmission eliminates inter-centre differences. MAGMA. 2006; 19:209–222. [PubMed: 16957936]
66. Vavasour IM, Whittall KP, Li DK, MacKay AL. Different magnetization transfer effects exhibited by the short and long T(2) components in human brain. Magn Reson Med. 2000; 44:860–866. [PubMed: 11108622]
67. Stanisz GJ, Webb S, Munro CA, Pun T, Midha R. MR properties of excised neural tissue following experimentally induced inflammation. Magn Reson Med. 2004; 51:473–479. [PubMed: 15004787]
68. Mottershead J, Schmierer K, Clemence M, Thornton J, Scaravilli F, Barker G, Tofts P, Newcombe J, Cuzner M, Ordidge R, McDonald W, Miller D. High field MRI correlates of myelin content and axonal density in multiple sclerosis: a post-mortem study of the spinal cord. J Neurol. 2003; 250:1293–1301. [PubMed: 14648144]

Europe PMC Funders Author Manuscripts

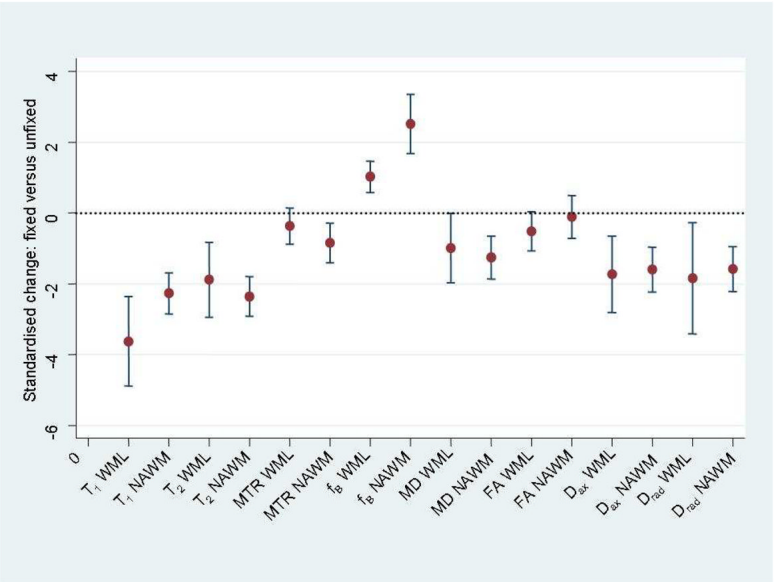

1. .

Mean changes (expressed as standard deviations from zero in unfixed tissue) with 95% confidence intervals of quantitative MR indices in *post mortem* multiple sclerosis brain following fixation. MTR= magnetisation transfer ratio, f_B= macromolecular proton fraction, MD= mean diffusivity, FA= fractional anisotropy, D_{ax}= axial diffusivity, D_{rad}= radial diffusivity, NAWM= normal appearing white matter, WML= white matter lesions.

Europe PMC Funders Author Manuscripts

Table 1

Comparison* of MR indices between lesions and normal appearing white matter (NAWM) in brain samples of patients with MS before and after fixation. Mean= mean of individual patient means (averaged across tissue sample), SD= standard deviation of these individual patient means, MTR= magnetisation transfer ratio, f_B= macromolecular proton fraction, MD= mean diffusivity, D_{ax}= axial diffusivity, D_{rad}= radial diffusivity [$mm^2s^{-1}\times 10^{-3}$], FA= fractional anisotropy.

			Lesions	NAWM
Index	**Condition**	**N cases**	**Mean (SD)**	**Mean (SD)**
T_1 [ms]	Unfixed	15	1207 (294)	681 (137)
	Fixed	14	748 (154)	377 (73)
T_2 [ms]	Unfixed	15	121 (13)	81 (8)
	Fixed	15	107 (12)	61 (5)
MTR [pu]	Unfixed	15	24.5 (2.3)	33.9 (2.8)
	Fixed	15	22.5 (3.8)	30.0 (3.7)
f_B [pu]	Unfixed	10	3.1 (1.3)	7.0 (2.1)
	Fixed	12	4.6 (1.5)	10.7 (2.6)
MD	Unfixed	13	0.36 (0.09)	0.22 (0.47)
	Fixed	15	0.31 (0.08)	0.16 (0.04)
D_{ax}	Unfixed	13	0.43 (0.12)	0.29 (0.05)
	Fixed	15	0.34 (0.08)	0.20 (0.04)
D_{rad}	Unfixed	13	0.34 (0.1)	0.2 (0.05)
	Fixed	15	0.29 (0.08)	0.15 (0.05)
FA	Unfixed	13	0.23 (0.06)	0.40 (0.14)
	Fixed	15	0.19 (0.05)	0.39 (0.12)

* All differences $p \leq 0.01$

Europe PMC Funders Author Manuscripts

Table 2

Comparison of MR indices before and after fixation in *post mortem* brain slices of patients with MS. Mean= mean of individual patient means (averaged across tissue sample), SD= standard deviation of these individual patient means, NAWM= normal appearing white matter, MTR= magnetisation transfer ratio, f_B= macromolecular proton fraction, MD= mean diffusivity, D_{ax}= axial diffusivity, D_{rad}= radial diffusivity [$mm^2s^{-1}\times 10^{-3}$], FA= fractional anisotropy.

			Unfixed	Fixed	
Index	**n cases**	**Region**	**Mean (SD)**	**Mean (SD)**	**p**
T_1 [ms]	14	Lesions	1196 (302)	748 (154)	<0.01
		NAWM	668 (131)	377 (73)	<0.01
T_2 [ms]	15	Lesions	121 (13)	107 (12)	<0.01
		NAWM	81 (8)	61 (5)	<0.01
MTR [pu]	15	Lesions	24.5 (2.3)	22.5 (3.8)	0.11
		NAWM	33.9 (2.8)	30.0 (3.7)	0.01
f_B [pu]	8	Lesions	3.0 (1.3)	4.3 (1.7)	0.03
		NAWM	7.1 (2.2)	10.8 (2.8)	<0.01
MD	13	Lesions	0.36 (0.1)	0.31 (0.1)	0.06
		NAWM	0.22 (0.1)	0.16 (0.04)	<0.01
D_{ax}	13	Lesions	0.43 (0.13)	0.35 (0.09)	0.01
		NAWM	0.29 (0.05)	0.2 (0.05)	<0.01
D_{rad}	13	lesions	0.35 (0.09)	0.3 (0.08)	0.03
		NAWM	0.2 (0.05)	0.15 (0.05)	<0.01
FA	13	Lesions	0.23 (0.1)	0.19 (0.1)	0.07
		NAWM	0.40 (0.1)	0.39 (0.1)	0.7

Europe PMC Funders Author Manuscripts

Magn Reson Med. Author manuscript; available in PMC 2008 February 13.

Table 3

Correlation* between variables in *post mortem* brain slices of patients with MS. MR indices were obtained in unfixed tissue. n= lesions/regions of normal appearing white matter included, MTR= magnetisation transfer ratio, f_b= macromolecular proton fraction, MD= mean diffusivity, FA= fractional anisotropy, D_{ax}= axial diffusivity, D_{rad}= radial diffusivity)

	T_2	T_1	MTR	f_B		MD	FA	D_{ax}	D_{rad}
T_1	*r*= 0.82				**FA**	*r*= −0.64			
	n= 51/15					n= 33/13			
MTR	*r*= −0.88	*r*= −0.79			**D_{ax}**	*r*= 0.84	*r*= −0.31 *1)*		
	n= 51/15	n= 51/15				n=33/13	n=33/13		
f_B	*r*= −0.8	*r*= −0.83	*r*= 0.83		**D_{rad}**	*r*= 0.94	*r*= −0.71	*r*= 0.82	
	n= 33/10	n= 33/10	n= 33/10			n=33/13	n=33/13	n=33/13	
T_{myelin}	*r*=0.82	*r*= 0.77	*r*= −0.83	*r*= −0.72	**T_{myelin}**	*r*= 0.73	*r*= −0.78	*r*= 0.53	*r*= 0.74
	n= 47/15	n= 47/15	n= 47/15	n= 31/10		n= 31/13	n= 31/13	n=31/13	n=31/13
Axon	*r*=−0.82	*r*= −0.63	*r*= 0.8	*r*= 0.67	**Axon**	*r*= −0.52	*r*= 0.58	*r*= −0.49	*r*= −0.55
count	n= 46/15	n= 46/15	n= 46/15	n= 30/10	**count**	n= 30/13	n= 30/13	n=30/13	n=30/13
$T_{gliosis}$	*r*= −0.37 *1)*	*r*= −0.54	*r*= 0.31 *1)*	*r*= 0.41 *1)*	**$T_{gliosis}$**	*r*= −0.4 *1)*	*r*= 0.5	*r*= −0.17 *1)*	*r*= −0.39 *1)*
	n= 47/15	n= 47/15	n= 47/15	n= 31/10		n= 31/13	n= 31/13	n=31/13	n=31/13

* p≤0.01 except for

1) (not significant).

Europe PMC Funders Author Manuscripts

Table 4

Correlation* between variables in *post mortem* brain slices of patients with MS. MR indices were obtained after fixation. n= lesions/regions of normal appearing white matter included, MTR= magnetisation transfer ratio, f_b= macromolecular proton fraction, MD= mean diffusivity, FA= fractional anisotropy, D_{ax}= axial diffusivity, D_{rad}= radial diffusivity, T= Transmittance.

	T_2	T_1	MTR	f_B	T_{myelin}	Ax count		MD	FA	D_{ax}	D_{rad}
T_1	*r*= 0.91						**FA**	*r*= −0.82			
	n= 43/14							n= 33/15			
MTR	*r*= −0.69	*r*= −0.54					**D_{ax}**	*r*= 0.96	*r*= −0.84		
	n= 44/15	n= 40/14						n=33/15	n=33/15		
f_B	*r*= 0.91	*r*= −0.87	*r*= 0.69				**D_{rad}**	*r*= 0.94	*r*= −0.85	*r*= 0.98	
	n= 35/12	n= 35/12	n= 35/12					n=33/15	n=33/15	n=33/15	
T_{myelin}	*r*= 0.92	*r*= 0.89	*r*= −0.68	*r*= −0.86			**T_{myelin}**	*r*= 0.78	*r*= −0.83	*r*= 0.8	*r*= 0.81
	n= 35/15	n= 38/14	n= 41/15	n= 32/12				n= 33/15	n= 33/15	n=33/15	n=33/15
Axon	*r*= −0.78	*r*= −0.78	*r*= 0.48	*r*= 0.61	*r*=−0.80		**Axon**	*r*= −0.53	*r*= 0.64	*r*= −0.49	*r*= −0.52
count	n= 40/15	n= 37/14	n= 40/15	n= 32/12	n= 46/15		**count**	n= 32/15	n= 32/15	n=32/15	n=32/15
$T_{gliosis}$	*r*= −0.45	*r*= −0.34 *1)*	*r*= 0.62	*r*= 0.52	*r*= 0.54	*r*= 0.2 *1)*	**$T_{gliosis}$**	*r*= −0.4 *1)*	*r*= 0.51	*r*= −0.45 *1)*	*r*= −0.45 *1)*
	n= 41/15	n= 38/14	n= 41/15	n= 32/12	n= 47/15	n= 46/15		n= 33/15	n= 33/15	n=32/15	n=32/15

*p≤0.01 except for

1)(not significant).

1)(p≤0.03).